



Hybrid RIME Optimization for Robust Feature Selection and Photovoltaic MPPT Under Complex Conditions

K Surya Teja¹, Immanuel Anupalli², P.Sudheer³

¹Research scholar, BEST Innovation University, suryatejabestiu2025@gmail.com

²Professor of EEE, Gayathri Institute of Technology and Management, anupalliimmanuel@gmail.com

³Professor of EEE, Sreenivasa institute of technology and management studies, psudheer35@gmail.com

Abstract:- Photovoltaic (PV) systems rely on maximum power point tracking (MPPT) to ensure optimal performance. The solar system's output characteristic curve has many peaks due to differences in temperature and light intensity, and the conventional MPPT algorithms accomplish unwell in multifaceted and dynamic scenarios. By integrating tent mapping during the initialisation phase, this study augments the algorithm's exploratory competences and presents a hybrid RIME Optimisation method to improve MPPT and feature selection tasks for PV systems operating in partial shading conditions. It also uses piecewise mapping to construct sequences that optimise the algorithm's parameters, so striking a fair balance between local exploitation and global exploration. From the perspective of feature selection, the hybrid approach reduces computational costs while improving classification accuracy by generating optimal subsets using metaheuristics inspired by nature. In the PV MPPT context, the proposed technique accomplishes better in relationship to the tracking speed, stability and accuracy than PSO-BOA, traditional RIME, and IRIME approaches.

Keywords: Feature Selection, RIME Optimization, Tent mapping, Logistic mapping, MPPT, PV Systems, Partial Shading condition.

1. Introduction

Photovoltaic energy systems have a lot of promise as a viable substitute for fossil fuels because they can generate power in a safe, long-lasting, and non-polluting way. Several improvements in solar technology have made PV modules much more efficient and less expensive in the last few years [1-2]. In some places, natural gas power and wind plants are cheaper than photovoltaic systems, which are the most expensive option in others [3]. Then, more research is needed to make PV systems more widely used. A solar energy system's efficiency is proportional to the power consumption of its PV modules. Additionally, the maximum power point (MPP) is the sole optimal location for a photovoltaic system to operate due to the non-linearity of the P-V curve. Environmental factors like temperature and irradiance have a big effect on where the MPP is on the P-V curve. Also, partial shading conditions (PSC), where buildings, trees, and clouds shade some modules in a series string, change the shape of the P-V curve and give uneven irradiances. This results in a single global MPP and multiple local ones on the P-V curve. Because of this, getting the maximum amount of energy is challenging.



MPPT technology is an important part of PV systems that makes sure that PV panels always give off the most electrical energy possible. There are two main types of MPPT algorithms: traditional ones and ones that use artificial intelligence [4-5]. Classical MPPT approaches include incremental conductance (INC), constant voltage (CV) tracking, and perturb and observe (P&O) which are frequently employed in applications where economic factors are significant, owing to their simplicity, reliability, and relative ease of implementation [6-7]. Elgendy et al. [8] created a P&O scheme which changes the voltage up or down every so often while the PV array is working to make the change in output power.

Adding incremental "perturbations" to determine if the method has hit its peak power point is the fundamental principle underlying the approach. After reaching its maximum, the system will keep oscillating around the MPP, which will cause instability and power outages. MPPT maintains a constant operating voltage relative to the open-circuit voltage, was expected to be achieved using the CV tracking methodology by Salameh et al. [9]. The INC methodology, which is grounded on the P&O, has a number of improvements, one of which is that it uses "conductance change" instead of "power change" to figure out which way the perturbation is going [10]. It is important to remember that these old methods don't work well in quickly changing weather and have poor tracking accuracy because of oscillations and bad tracking.

Artificial intelligence optimisation methods are very popular in the MPPT industry because they can optimise things all over the world [11–12]. Due to its simplicity and ease of use, the particle swarm optimisation (PSO) approach has gained popularity in MPPT. It works by imitating how groups of birds et al. [13–14]. By mimicking the behaviour of a butterfly population as it searches for food, the butterfly optimisation algorithm (BOA) is able to quickly identify a good solution [15-16]. To address the issue of slow convergence in the BOA method and improve optimisation outcomes in the MPPT system, the particle swarm-butterfly optimisation algorithm (PSO-BOA) combines the best aspects of the PSO algorithm and other relevant methods [17]. However, changes in the search range could affect these smart algorithms, which would change how accurately the population tracks. Also, because they converge slowly, they might not be able to quickly adapt to changes in the environment, which would limit how much power they can produce.

On top of that, a lot of people have worked on improving the algorithms so that maximum power points can be tracked more accurately. In an effort to resolve the issue of proton exchange membrane fuel cell stacks' nonlinear power output, Touti, E. et al. [18] explored different MPPT approaches based on metaheuristic optimisation. The most effective and powerful cuckoo search method in the simulation was CDSV with CSM, which uses continuous slope values. Investigated the operation of a solar PV system in various scenarios by simulating and comparing MPPT algorithms grounded on PSO[19], genetic algorithm (GA),



bat optimisation, and grey-wolf optimisation (GWO). According to the outcomes, GWO model outperformed the other optimisation techniques with an MPPT efficiency of 98%.

Out of all the MPPT optimisation algorithms tested, the tracking efficiency achieved by the salp swarm optimisation algorithm (SSOA) was 98.38%. for solar PV systems operating in partial shade [20]. Another method used in this study was a convolutional neural network (CNN) model, which achieved a 94.11% success rate in classifying PV system problems. To assess the effectiveness of multiple MPPT algorithms under varying solar irradiation conditions, researchers used Matlab Simulink to simulate a PV system with a single diode [21]. Comparing the IRIME optimisation approach to RIME and PSO-BOA, the simulation results reveal that it achieves a tracking accuracy of over 98.88%. Wang, Y. et al. [22] put forward the improved IRIME optimisation method for PV system MPPT technology in a range of different environmental conditions. But the selection process described above could cause early convergence in optimisation environments that are very complicated. In order to improve maximum power point tracking (MPPT) and feature selection tasks for photovoltaic (PV) systems operating in partial shade, this study introduces a hybrid RIME Optimisation method that incorporates tent mapping during the initialisation phase. This improves the algorithm's exploratory capabilities. By optimising the algorithm's parameters by piecewise mapping, it achieves a happy medium between local exploitation and global exploration.

2. Photovoltaic (PV) System Modelling

Because it converts solar radiation into usable electricity, PV power generation systems rely heavily on the PV module. Absorbing photon energy separates the charges and causes the electrons in the semiconductor material to migrate; this is the major method it works. Through an external circuit, the charges build up to a current that converts light energy into electrical energy. Figure 1 shows the exact structure of a PV module, which, if all goes according to plan, may be reduced to a perfect diode and a constant current source.

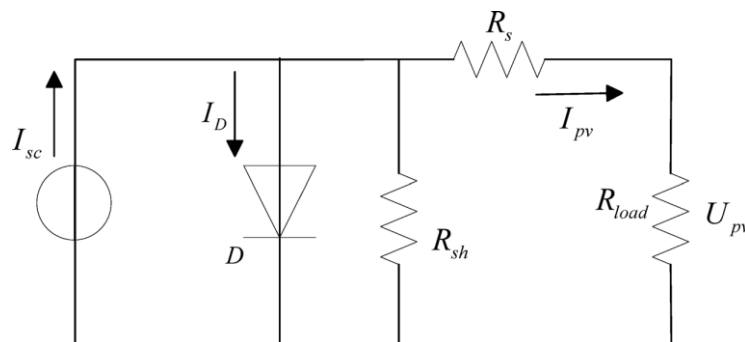


Fig.1: Circuit based on the single diode model

In the Fig.1, I_{sc} stands for the current that excites photonics., I_D shows the diode's reversal current, R_s signifies series resistance, shunt resistance represented by R_{sh} , and R_{load} refers to



the external load of the PV panel. In accordance with Kirchhoff's Law, I_{pv} and U_{pv} were determined by the equations (1) and (2), respectively, which stand for the voltage and current produced by the PV system.

$$I_{pv} = I_{sc} - I_D - I_{sh} \quad \dots(1)$$

$$U_{pv} = U_D - I_{pv} \times R_s \quad \dots(2)$$

I_{sh} =Current leaking through in parallel, more precisely the current draining through R_{sh} , which is from the highest point to the lowest, while U_D indicates the inverse voltage. I_D = diode's reversal current, represented by Equation (3):

$$I_D = I_o * \left[\exp\left(\frac{U_D}{U_T}\right) - 1 \right] = I_o * \left[\exp\left(\frac{q(U_{pv} + I_{pv}R_s)}{nkT}\right) - 1 \right] \quad \dots(3)$$

I_o = Diode's reverse saturation current and the term U_T , defined as knT/q , represents the thermoelectric potential, where q signifies the charge of an electron, i.e., 1.6×10^{-19} C. The variable 'n' refers to the exponent of the diode, which generally falls within the range of 1 to 2. Equation (4) is obtained by plugging the given values into the initial formula (1) in the following way:

$$I_{pv} = I_{sc} - I_o * \left[\exp\left(\frac{q(U_{pv} + I_{pv}R_s)}{nkT}\right) - 1 \right] - \frac{U_{pv} + I_{pv}R_s}{R_{sh}} \quad \dots(4)$$

PV characteristic curves under different conditions

Light, temperature, and other external variables can significantly affect the nonlinear output characteristics of photovoltaic arrays. The characteristic curves of the current and voltage for photovoltaic arrays at various temperatures and irradiation levels are displayed in Figure 2. The open-circuit voltage gradually decreases with increasing temperature. The OC voltage is rather consistent regardless of the irradiance, while the SC current fluctuates as the irradiance increases. The total maximum power output usually goes up when the irradiance goes up and down when the temperature goes up. When evaluating and using PV arrays, it's important to think carefully about how changes in temperature and irradiance in the outside world affect them because they have such a big effect.

Under operational conditions, the outside world always causes partial shading of photovoltaic (PV) arrays. Affected PV modules' output voltage and current are reduced as a result. Also, the two terminals on the output cable act as loads because their potentials are lower. If these conditions last for a long time, the shaded photovoltaic modules may get very hot, which could damage the photovoltaic parts. Shade prevents current from damaging the diode in the photovoltaic module. To increase the voltage output, it is required to connect each PV module in series. Join many modules in succession to create strings. Then, to boost the system's total current output, connect those modules in parallel. This method makes sure that the PV array is



securely installed and also greatly improves the system's overall efficiency, which leads to more power being produced.

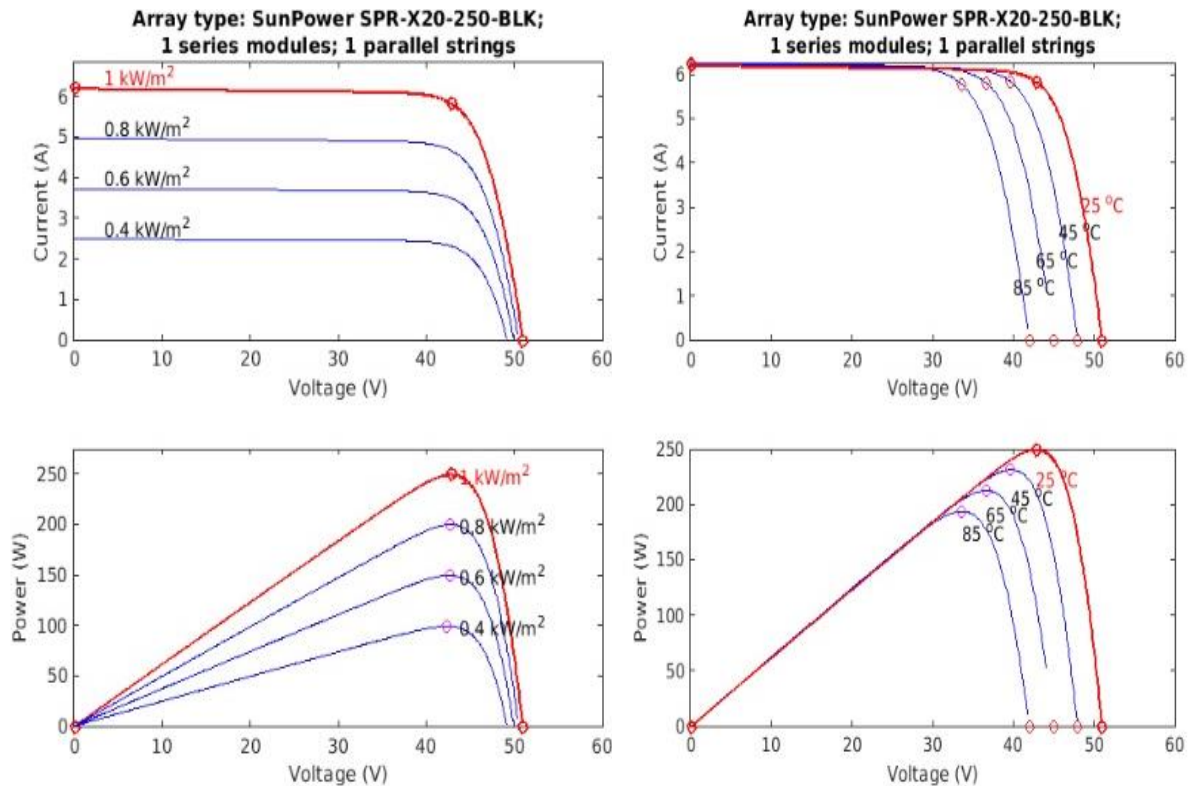


Fig.2: (a). Under different irradiance conditions (b). Under different temperature conditions

Figure 2(a) shows that the photovoltaic array works under normal conditions with even lighting. The light level stays at 1,000 lx, and the temperature stays at 25 °C. Under these standard conditions, the photovoltaic system's output characteristics show a unimodal pattern, being limited to a single MPP, called P1, as shown in case 1 of Figure 4.

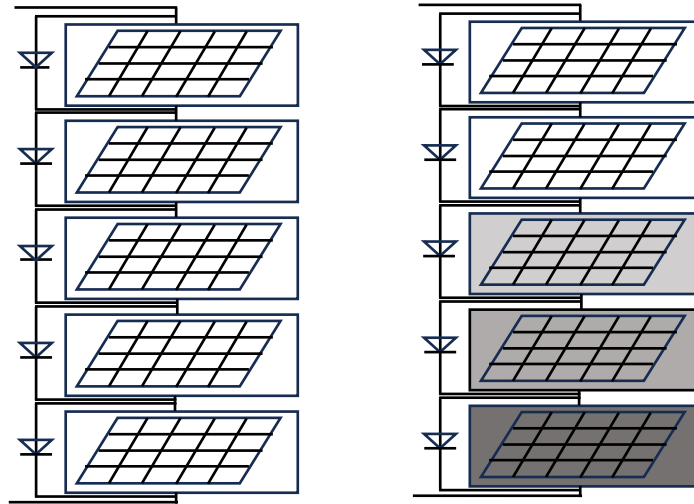
The output P-V curves have different peak features because each PV module gets a different amount of irradiance while the system is running. Table 1 shows the specific operating conditions for partial shading conditions (PSC), which are shown in Fig. 2 (b). Here, two of the solar panels receive equal light, the other three panels experience erratic of shade. In case 2 of Fig. 4, P3 is the GMPP, and P2 and P4 are the LMPP, as shown. Standard MPPT techniques often get wedged at local best P4, which causes power loss, and they can't tell the difference between P3 and P4 when looking at certain P-V characteristics. Also, having more LMPPs could make the global tracking performance of standard methods much worse. So, it is very important to make a GMPPT device that works well and is efficient.



Received: 16-09-2025

Revised: 05-10-2025

Accepted: 11-11-2025



a). Under constant illumination b). When subjected to partial shade

Fig.3: PV array structure with five series modules

Table 1: PV panels at different operating conditions

Case	Temp(°C)	S ₁ (W/m ²)	S ₂ (W/m ²)	S ₃ (W/m ²)	S ₄ (W/m ²)	S ₅ (W/m ²)
1	25	1000	1000	1000	1000	1000
2	25	1000	1000	800	700	600

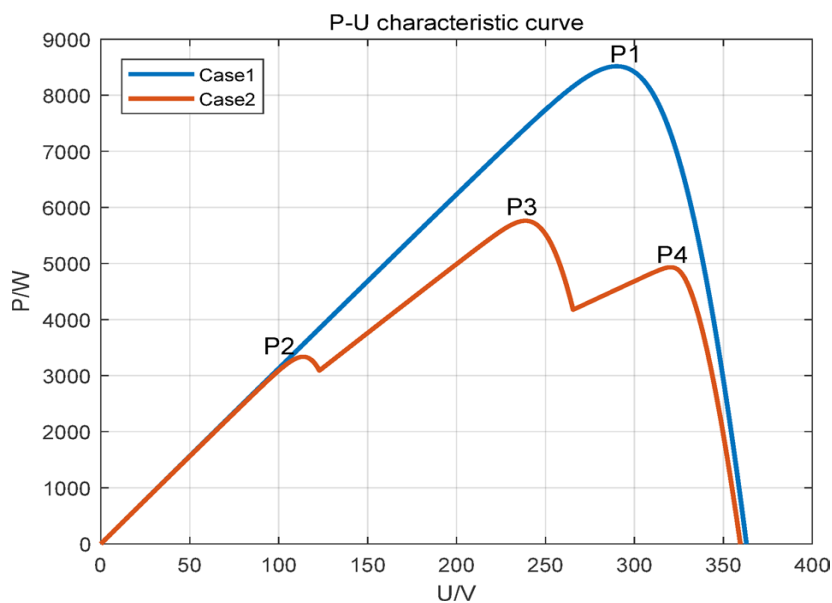


Fig.4: P-V characteristic curve under normal and PSC condition



3. MPPT based on HRIME

The RIME algorithm is a smart optimisation tool that combines the best parts of both intelligent and traditional algorithms. It can reach its goals of high accuracy and quick response thanks to its great global search abilities and adaptive adjustment methods.

RIME optimization algorithm

There are two kinds of frost ice that can happen in different situations: soft frost and hard frost. The RIME algorithm gets its idea for exploration and exploitation from the growth mechanism. Wind speed and airflow are two examples of environmental factors that slow down the growth of rime ice. As shown in Fig. 5, growth will stop when conditions become stable.

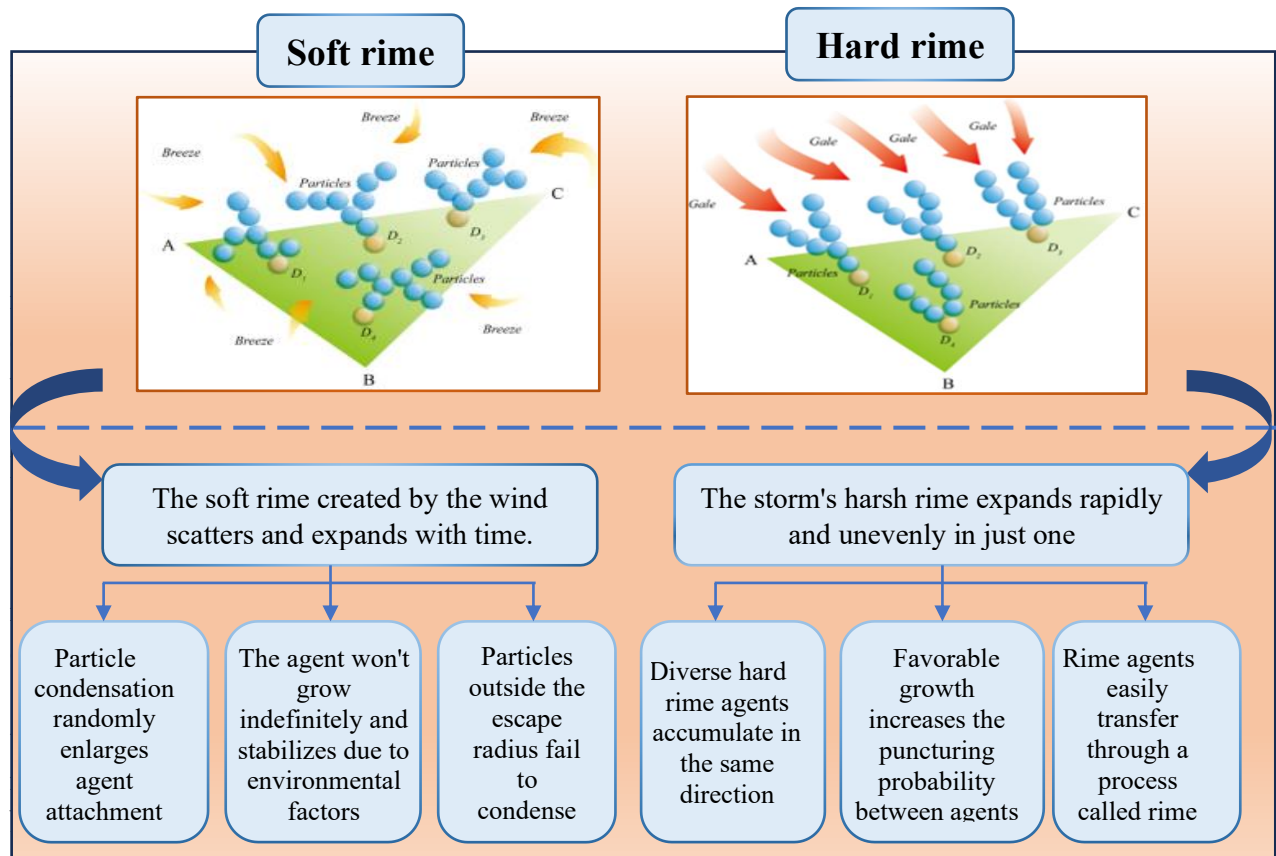


Fig.5. Different factors cause soft rime and hard rime to form.

Soft Rime (SR) occurs in places with gentle breezes, the wind speeds are low and the direction changes often, which makes the growth slow and the structure random. On the other hand, Hard Rime (HR) forms quickly and grows in a direction that stays mostly the same. It happens when the wind is blowing quickly and in the same direction in the same flat area. When all the parts of the RIME work together, there are four steps: initialising the rime cluster, using the SR search strategy, HR puncture, and the Positive Greedy Selection (PGS) approach.



Initialization of RIME cluster

Initially, in RIME starting places of particles are set up by arbitrarily generating them. The full rime-population (called R) is made up of different rime-agents (called S_m), where m is the rime agents sequential number. Each S_m is made up of several rime-particle (called x_{mn}), where, n is the rime particles number in order. The whole population of hoarfrost R is initialised at the outset, as clearly shown in Eq. (5):

$$R = \begin{bmatrix} x_{11} & x_{12} \cdots & x_{1n} \\ \vdots & \ddots & \vdots \\ x_{m1} & x_{m2} \cdots & x_{mn} \end{bmatrix} \quad \dots(5)$$

In the matrix, each row represents to a "rime-agent," as a result of which every column is a "rime-particle." $F(S_m)$ shows how each "rime-agent" S_m , is improving, which is linked to the meta-heuristic algorithm's fitness value. The fitness value $F(S_m)$ serves to assess the presentation of each agent, as illustrated in the subsequent Equation (6):

$$F(S_m) = \begin{bmatrix} f([x_{11} & x_{12} \cdots & x_{1n}]) \\ \vdots & \ddots & \vdots \\ f([x_{m1} & x_{m2} \cdots & x_{mn}]) \end{bmatrix} \quad \dots(6)$$

Search strategy of soft-rime

By capitalising on high dispersion and randomness of crystalline ice under a mild wind setting, the soft frost search approach is put into action. This method lessens the chances of particles being stuck in local optima by making sure they efficiently cover the whole search area during the initial rounds. The calculation of θ via eq.(7) has an effect on the particle's directional motion.

$$\theta = \pi \cdot \frac{t}{10.T} \quad \dots(7)$$

Here, t denotes the number of iterations now being performed, whereas T is the maximum iterations that the algorithm can handle. The environmental component β ensures that the algorithm will converge, as described in Eq. (8), by simulating the influence of external conditions.

$$\beta = 1 - \frac{\left[\frac{\gamma \cdot t}{T} \right]}{\gamma} \quad \dots(8)$$

Here, γ gearshifts the amount of sectors in the step function, and the symbol $[\cdot]$ designates the skirting operation. As seen in Eq. (9): the likelihood of people clustering is affected by the attachment coefficient E, which increases as the iteration count increases:



$$E = \sqrt{\left(\frac{t}{T}\right)} \quad \dots(9)$$

The crusade characteristics of hoarfrost ice particles are represented by their position as indicated in Equation (10):

$$R_{ij}^{new} = R_{best,j} + r_1 \cdot \cos \theta \cdot \beta \cdot (h \cdot (Ub_{ij} - Lb_{ij}) + Lb_{ij}), \quad \text{if } r_2 < E \quad \dots(10)$$

In this case, i, j stands the j^{th} element that is linked to the i^{th} rime-agent, and R_{ij}^{new} shows the modernized particle. $R_{(best,j)}$ is the j^{th} component of the optimal rime-agents population R . As shown in Eq. (7), the parameter r_1 , which is a random number between -1 and 1, along with $\cos\theta$, which will change after a certain number of iterations, affects the direction of particle movement. As per Eq. (8), the environmental factor, β , is used to make sure the algorithm converges and counts the number of iterations to show how the outside world affects the algorithm. The remoteness among the centres of two rime elements is determined by the degree of adhesion, that can take on values between 0 and 1.

$$R_{new} = \begin{cases} R_{best} & r_3 < f^g(S_m) \\ R_{new} & \text{Otherwise} \end{cases} \quad \dots(11)$$

4. Hybrid RIME optimization

The RIME algorithm now has a strong selection process instead of a random one, thanks to the tent mapping algorithm's strong selection mechanism. This change improves exploration-exploitation balance to drive the search away from local optima and towards the global optimal solution.

Tent mapping:

The tent map has a simple computational formula that makes it easy and efficient to use. The tent map uses a chaotic sequence that is evenly spread out to cover the search space of RIME more evenly. Also, RIME lowers the chance of local optima by starting with a diverse population and only a few control parameters, which is different from other chaotic maps. The improvements have a direct effect on how well the fault detection system works, making it more reliable and accurate by creating a clear and useful link with the system. A tent map shows how chaotic behavior can lead to very accurate results. The equation below shows the chaotic sequence phrases that are part of this function:

$$x_{k+1} = \begin{cases} \frac{x_k}{a}, & 0 \leq x_k < a \\ \frac{1-x_k}{a}, & a \leq x_k \leq 1 \end{cases} \quad \dots(12)$$

In this scenario, where a is set to 0.5, the tent map produces chaotic sequences within the interval (0, 1).



Piecewise mapping

The three numbers r_1 , r_2 , and r_3 are generated by RIME using a uniform distribution. This has the potential to impact the global search capacity and cause values to be uneven. Chaos theory is used to make the algorithm more random and easier to follow. It does this by using piecewise mapping to make chaotic sequences for the parameters r_1 , r_2 , and r_3 . In order to reduce the possibility of RIME convergent to local optima, this technique comprises shifting the locations of home-grown solutions. The piecewise chaotic mapping is a fragmented form of the mapping function. In equation (13) we have the chaotic mapping formula:

$$y_{k+1} = \begin{cases} \frac{x_k}{p}, & 0 \leq x_k < p \\ \frac{x_k - p}{0.5 - p}, & p \leq x_k < 0.5 \\ \frac{1 - p - x_k}{0.5 - p}, & 0.5 \leq x_k < 1 - p \\ \frac{1 - x_k}{p}, & 1 - p \leq x_k < 1 \end{cases} \quad \dots(13)$$

In this case, x_k stands for the values that come from random iteration, and the piecewise function is divided into four smaller sub-functions by the piecewise control factor p . According to the results of the experiments, a parameter value of 0.3 yields the best performance. Due to this, the article concludes that $p = 0.3$. The random number function creates an initial value x_k that is a random number between 0 and 1. After that, three iterations are run. The value of x_{k+1} is found by using the value of x_k from the last iteration. The results of the second, third, and fourth iterations names of the iterative results are assigned to r_1 , r_2 , and r_3 , respectively.

MPPT based on hybrid RIME

The RIME MPPT finds the maximum power point for solar systems fast, correctly, and consistently by combining the tent mapping process during initialisation with the robust global search features of the RIME and IRIME algorithms. Hybrid RME's flowchart is exposed in Figure 6.

1. First, the RIME algorithm's settings are set up, and the tent method is used to find out where N people are. This method makes the algorithm better at searching the whole world by stopping the initial population from gathering in small groups.
2. The locations of the frost particles are constantly changing based on how easily they can move. The sine cosine algorithm uses r_1 to control the movement amplitude of candidate solutions, which helps balance the need for early global exploration with the need for later local exploitation. To find better solutions, detailed searches are done around the current best solution using the r_2 sequence that was made.
3. The program is then changed so that particles can move through the frostbite penetration mechanism. The segmented mapping's r_3 sequence expedites the process of finding the global optimum and fortifies the strategy behind the best solution that is currently available.



4. Lastly, using the PGS approach, compared the new fitness values to the prior ones, ensuring optimal results every time.

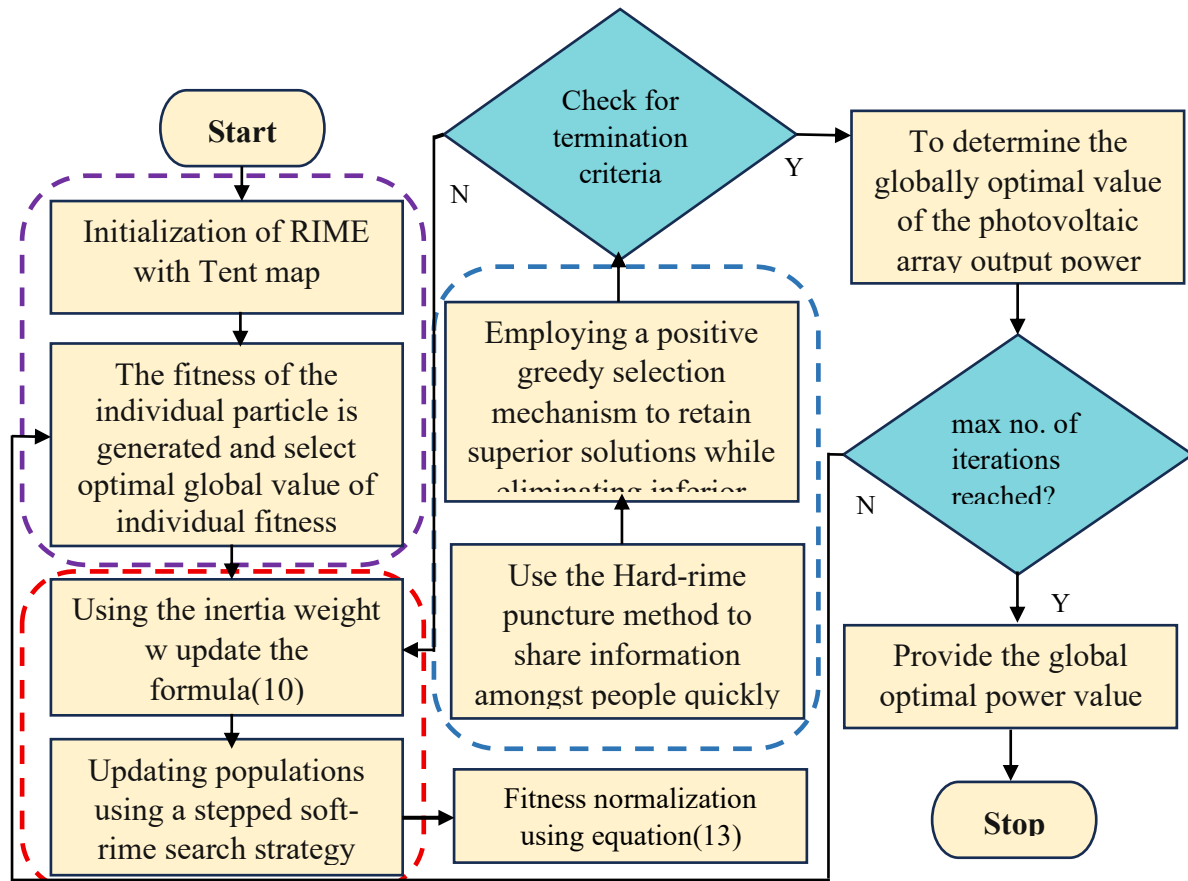


Fig. 6: Hybrid RIME algorithm flowchart

5. Results of the MPPT simulation under a uniform lighting condition:

The readiness of the anticipated IRIME optimisation technique in MPPT was tested using the simulation model. A constant distribution of light and shade is depicted in the model. Underneath these circumstances, tests are steered to examine and compare the results of HRIME with IRIME, RIME, and PSO-BOA. Parameter values for all of the algorithms in Table 2 down below.

Table 2: Solar Cell manufacturing specifications

S.No	Parameter Name	Set point
1	Cells per module	60
2	OC voltage (V_{oc})	37.2V
3	SC current (I_{sc})	9A

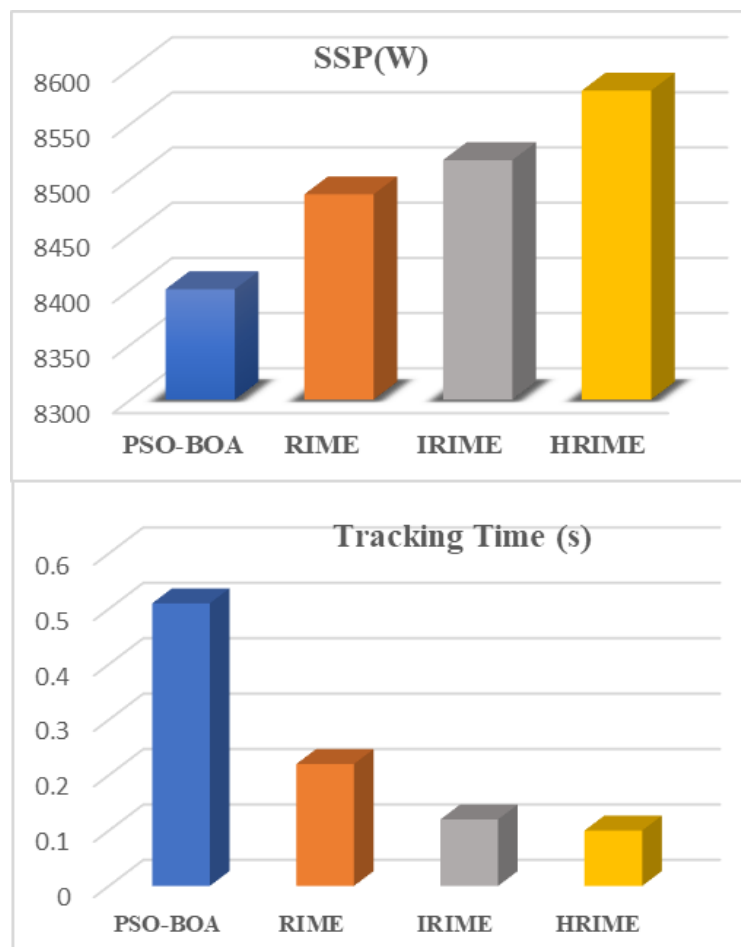


4	MPP voltage (V_{mp})	28.6V
5	MPP current (I_{mp})	7.65A
6	MPP setting value	218.79W

Table 3: Comparative results of SSP and Tracking Time.

S.No	Method	SSP(W)	Tracking Time (s)
1	SO-BOA	8400	0.51
2	RIME	8486	0.22
3	IRIME	8517	0.12
4	HRIME	8580	0.1

The artificial lighting setup for the simulation experiment is 1,000 W/m² with a constant temperature of 25°C. In this examination, we will compare the four methods that were before covered. According to the findings, the suggested HRIME algorithm outperforms the preliminary RIME, IRIME, and PSO-BOA approaches, particularly in relationship to steady state tracking power and tracking time.





Received: 16-09-2025

Revised: 05-10-2025

Accepted: 11-11-2025

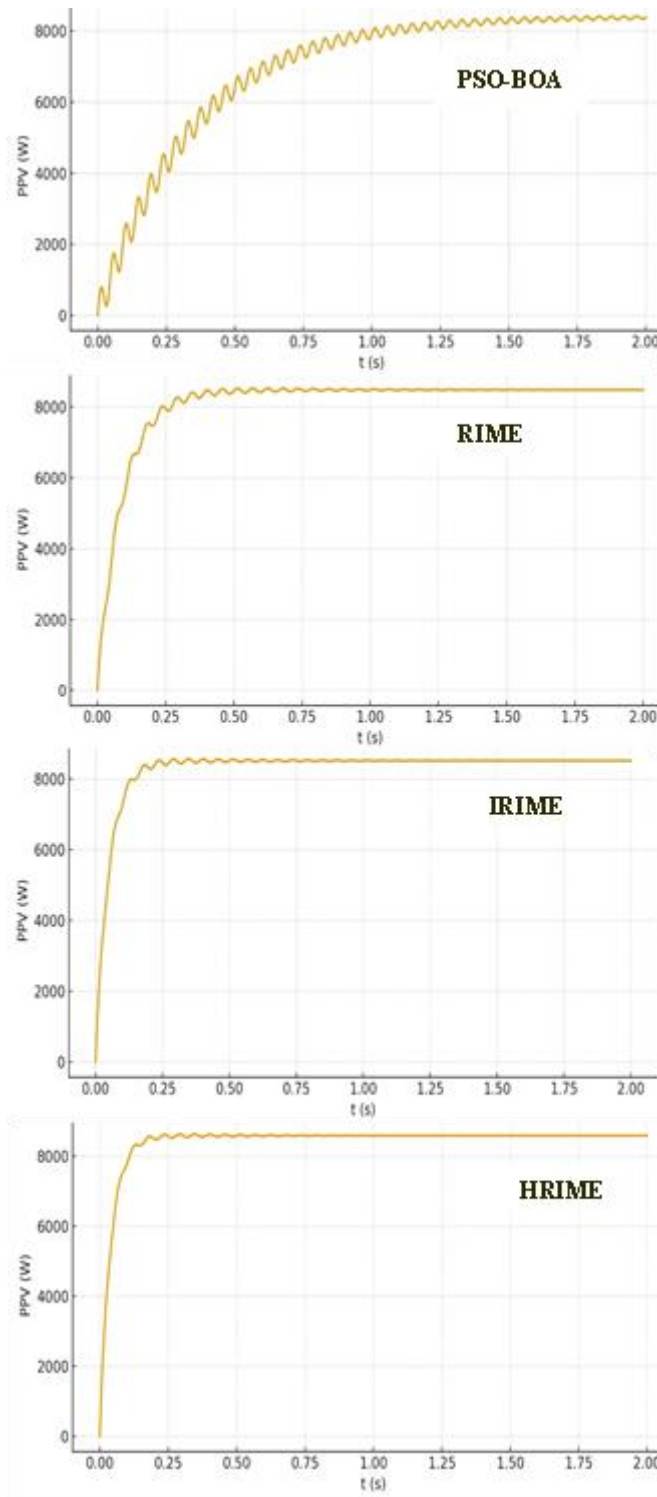


Fig. 7: Findings from different algorithms' simulations run under a consistent lighting scenario



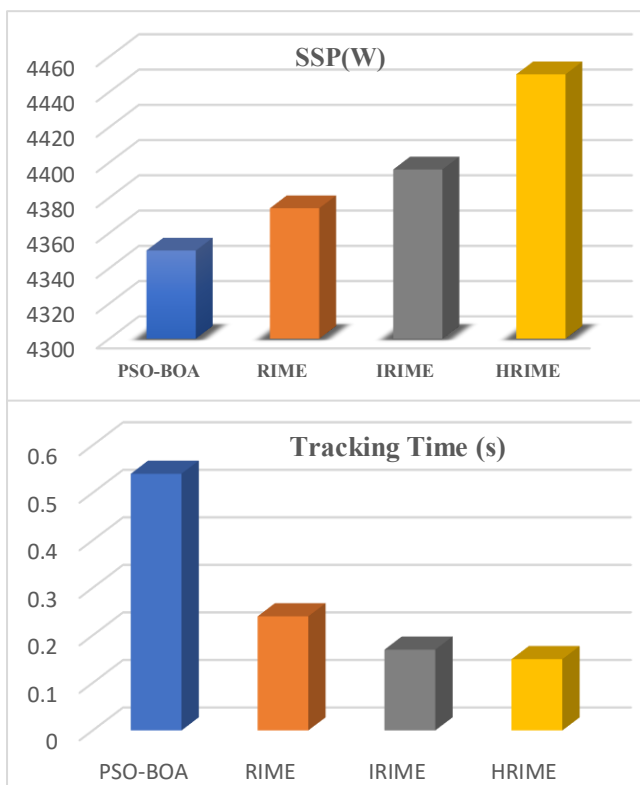
MPPT simulation optimization results under partial shading condition.

The temperature remains persistent at 25°C , simulation experiment is carried out under partially shaded settings. Irradiance levels of 1,000w/m2, 800w/m2, 700w/m2, and 600w/m2 are established for five PV panels at 0.6 seconds. Figure 8 and Table 4 display the results of the simulation that ran for 2 seconds after the GMPP.

Table 4: Comparative results of SSP and Tracking Time under partial shading condition.

S.No	Method	SSP(W)	Tracking Time (s)
1	PSO-BOA	8400	0.51
2	RIME	8486	0.22
3	IRIME	8517	0.12
4	HRIME	8580	0.1

The results demonstrate that the suggested HRIME surpasses the RIME, IRIME, and PSO-BOA approaches in relation to tracking duration and steady-state tracking power. The suggested HRIME algorithm outpaces IRIME, RIME, and PSO-BOA in terms of tracking time reduction.





Received: 16-09-2025

Revised: 05-10-2025

Accepted: 11-11-2025

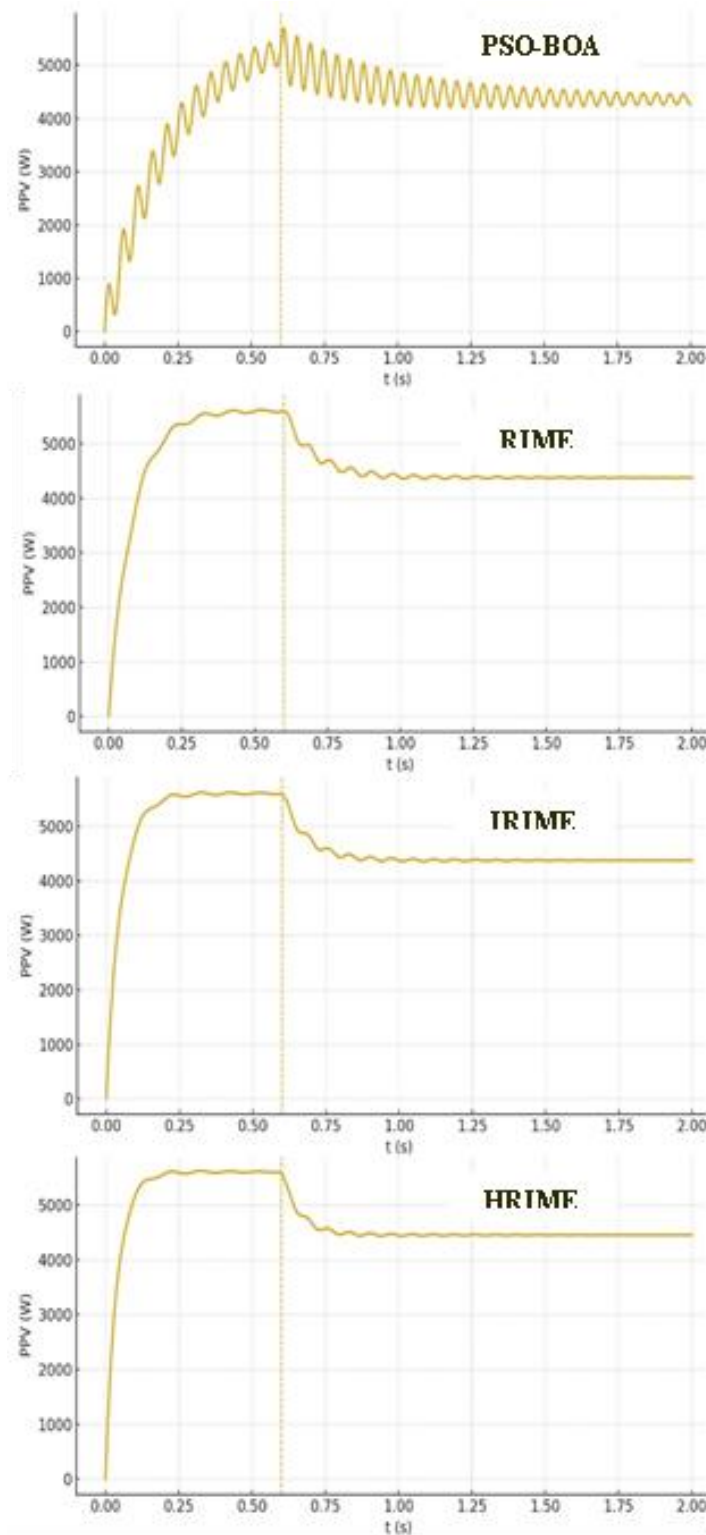


Fig. 8: Findings from different algorithms' simulations run under a variable lighting scenario



6. Conclusions:

This research is the inaugural application of the RIME optimisation algorithm to MPPT technology during PSC, facilitating precise pursuing the GMPP amidst a power–voltage curve characterised by multiple peaks. We present a tent mapping initialisation strategy to address the issues associated with the traditional RIME algorithm, including slow convergence and premature convergence to local optima. This makes it easier to move through the algorithm and lets you look over the search space more closely. Also, piecewise mapping is used to make sequence generation better and change algorithm parameters on the fly, which makes the system more flexible and adaptable. It also has an inertia weight that changes based on the iteration process. This speeds up convergence, cuts down on pointless blind searches, and improves the balance between local exploitation and global exploration. The proposed HRIME algorithm not only makes tracking more accurate and flexible, but it also makes the system run faster, smoother, and better overall.

References

- [1] S. Kurtz et al., “Historical analysis of champion photovoltaic module efficiencies,” *IEEE J. Photovolt.*, vol. 8, no. 2, pp. 363–372, Mar. 2018.
- [2] V. Benda, “Photovoltaics towards terawatts—Progress in photovoltaic cells and modules,” *IET Power Electron.*, vol. 8, no. 12, pp. 2343–2351, 2015, doi: 10.1049/iet-pel.2015.0102.
- [3] M. Malinowski, J. I. Leon, and H. Abu-Rub, “Solar photovoltaic and thermal energy systems: Current technology and future trends,” *Proc. IEEE*, vol. 105, no. 11, pp. 2132–2146, Nov. 2017.
- [4] Li, G. et al. Application of bio-inspired algorithms in maximum power point tracking for PV systems under partial shading conditions—A review. *J. Renew. Sustainable Energy Reviews*. 81, 840–873 (2018).
- [5] Sun, C., Ling, J. & Wang, J. Research on a novel and improved incremental conductance method. *J. Sci. Rep.* 12 (1), 15700 (2022).
- [6] Mao, M. et al. Classification and summarization of solar photovoltaic MPPT techniques: A review based on traditional and intelligent control strategies. *J. Energy Rep.* 6, 1312–1327 (2020).
- [7] Mohapatra, A. et al. A review on MPPT techniques of PV system under partial shading condition. *J. Renew. Sustainable Energy Reviews*. 80, 854–867 (2017).
- [8] Elgendy, M. A., Zahawi, B. & Atkinson, D. J. Assessment of perturb and observe MPPT algorithm implementation techniques for PV pumping applications. *J. IEEE Trans. Sustainable Energy*. 3 (1), 21–33 (2011).
- [9] Salameh, Z. M., Dagher, F. & Lynch, W. A. Step-down maximum power point tracker for photovoltaic systems. *J. Solar Energy*. 46 (5), 279–282 (1991).



- [10] Al-Dhaifallah, M. et al. Optimal parameter design of fractional order control based INC-MPPT for PV system. *J. Solar Energy*. 159, 650–664 (2018).
- [11] Moghassemi, A. et al. Two fast metaheuristic-based MPPT techniques for partially shaded photovoltaic system. *J. Int. J. Electr. Power Energy Syst*. 137, 107567 (2022).
- [12] Soufyane, Benyoucef, A. et al. Artificial bee colony based algorithm for maximum power point tracking (MPPT) for PV systems operating under partial shaded conditions. *J. Appl. Soft Comput*. 32, 38–48 (2015).
- [13] Yao, J. et al. Research on hybrid strategy particle swarm optimization algorithm and its applications. *J. Sci. Rep*. 14 (1), 24928 (2024).
- [14] Lynn, N. & Suganthan, P. N. Heterogeneous comprehensive learning particle swarm optimization with enhanced exploration and exploitation. *J. Swarm Evolutionary Comput*. 24, 11–24 (2015).
- [15] Tiwari, A. & Chaturvedi, A. A hybrid feature selection approach based on information theory and dynamic butterfly optimization algorithm for data classification. *J. Expert Syst. Appl*. 196, 116621 (2022).
- [16] Long, W. et al. Parameters identification of photovoltaic models by using an enhanced adaptive butterfly optimization algorithm. *J. Energy*. 229, 120750 (2021).
- [17] Achouri, F. et al. Structural health monitoring of beam model based on swarm intelligence-based algorithms and neural networks employing FRF. *J. J. Brazilian Soc. Mech. Sci. Eng*. 45 (12), 621 (2023).
- [18] Touti, E. et al. A comprehensive performance analysis of advanced hybrid MPPT controllers for fuel cell systems. *Sci. Rep*. 14, 04–24 (2025).
- [19] Senthilkumar, S. et al. Analysis of single-diode PV model and optimized MPPT model for different environmental conditions. *J. International Transactions on Electrical Energy Systems* 2022(1), 4980843 (2022).
- [20] Senthilkumar, S. et al. Nature-inspired MPPT algorithms for solar PV and fault classification using deep learning techniques. *Discover Appl. Sci*. 7, 31 (2025).
- [21] Senthilkumar, S. et al. Optimized Maximum Power Point Tracking Algorithm for Solar Photovoltaic with Dissimilar Environmental Conditions. 7th International Conference on I-SMAC (IoT in Social, Mobile, Analytics and Cloud) (I-SMAC). Kirtipur, Nepal, 2023, pp, 1061–1068. (2023).
- [22] Wang, Y., Zhang, W., Ma, Y. et al. An improved RIME optimization algorithm based maximum power point tracking method for photovoltaic system under partially shading condition. *Sci Rep* 15, 19507 (2025). <https://doi.org/10.1038/s41598-025-01586-y>.
- [23] S. Mirjalili, “SCA: A sine cosine algorithm for solving optimization problems,” *Knowl.-Based Syst.*, vol. 96, pp. 120–133, Mar. 2016.